# Back-Scatter by Oblate Ice Spheroids

DAVID ATLAS

*Geophysics Research Directorate, Air Force Cambridge Research Laboratories*

AND RAYMOND WEXLER

*Allied Research Associates, Inc., Concord, Mass.*

(Manuscript received 16 July 1962, in revised form 8 November 1962)

ABSTRACT

Back-scatter measurements are presented for a set of oblate ice spheroids and a set of ice-simulating dielectric spheroids at both 3.2- and 9.7-cm wavelengths as a function of aspect and polarization. The data are highly complex and not subject to simple generalizations. The only regular behavior is shown by particles whose major axes are smaller than about $\lambda/4$. This is approximately the upper size limit to which the simple Gans theory is applicable. For these small particles the cross section is a function only of the maximum linear dimension in the direction of polarization; thus, for polarization parallel to the major axis, the back-scatter is independent of aspect. However, as the particle axis/diameter ($b/a$) ratio decreases, the cross section relative to an equivolume sphere increases. For polarization perpendicular to the major axis, the cross section decreases from a maximum on the large face to a minimum on the small face. As $b/a$ decreases, the small face cross section continually decreases below that of an equivolume sphere.

For $D/\lambda \cong 0.5$, large (circular) face cross sections are generally enhanced (with respect to equivolume spheres); small face cross sections are usually degraded, the more so the smaller $b/a$. The situation is reversed only for $b/a > 0.8$. As with the smaller particles, polarization parallel (to the major axis) is superior to perpendicular polarization. When $D/\lambda > 0.5$ the large face cross sections tend to follow that indicated by geometric optics, with enhancement usually occurring for $b/a > 0.7$, but oscillating between enhancement and degradation for smaller $b/a$'s. Small face cross sections are usually equal to or less than those of equivolume spheres in this size regime, and in contrast to the small sizes, perpendicular polarization is superior to parallel for $b/a > 0.5$. In exceptional cases, the small face cross sections are enhanced, but only by a few decibels. Thus, unless wetting effects are important, it is not possible to attribute extraordinarily large reflectivities of hailstorms to shape and orientation phenomena.

The cancellation ratios to be expected upon switching from linear to circular polarization cover a broad range, overlapping that found for rainfall. Thus, polarization switching is not likely to provide a general means of distinguishing dry, oriented, oblate hail from rain. When the particles are water coated, polarization switching would be more useful. However, any tendency toward random orientation would diminish the polarization effects.

## 1. Introduction

As a result of the heightened interest in the physics and radar detection of hailstorms in recent years, the problem of the back-scatter from large ice spheres has received extensive attention. The experimental data of Atlas *et al.* (1960), which have since been confirmed by the theoretical calculations of Herman and Battan (1961, *a*, *b*) showed that ice spheres equal to or larger than about 1.5 wavelengths in diameter scatter more than ten times as well as metal ones of the same size. With these large cross sections it now becomes possible to explain some of the larger reflectivities associated with 3.2-cm echoes from hailstorms (Donaldson, 1961) with physically reasonable quantities of hail. However, the largest recorded reflectivities still require hail concentrations on and beyond the border of reality. Since many hailstones are oblate spheroids rather than spheres, the question arises as to whether or not such particles scatter better than equivolume spheres. Furthermore, the cross sections of such particles will generally depend on aspect with respect to the directions of propagation and polarization. This behavior must be determined if radar observations of precipitation in general, and of hail in particular, are to be interpreted correctly.

The theory for the scattering by an ellipsoid of arbitrary electromagnetic constants and orientation with respect to the incident field has been developed by Stevenson (1953) in a form suitable for numerical computation. However, Mathur and Mueller (1955) have noted that Stevenson's solution converges only for $\alpha = (2\pi a/\lambda) \lesssim 0.95$. When the dimensions of the ellipsoid are small with respect to the wavelength, use may be made of the Gans (1912) approximation. Calculations according to the Gans theory have been made by Atlas, Kerker and Hitschfeld (1953) for ice and water ellipsoids. Labrum (1953) has extended the Gans theory to confocal ellipsoids of different refractive index, as might be applicable to the case of water coated ice. In the extremes (all ice or all water) his calculations agree

Unauthenticated | Downloaded 06/28/22 12:35 AM UTC

with those of Atlas *et al.* for ice and water. In order to obtain data beyond the size range of the available theory, we have undertaken an experimental program to measure the cross sections of oblate spheroids of ice and an ice-simulating dielectric. A limited number of measurements of the back-scatter from oblate spheroids comprised of plexiglass have previously been reported by Harper.[1] However, the difference in refractive index between plexiglass ($m=1.61$) and ice ($m=1.78$), and the restriction of the measurements to a single size, casts some doubt on their general applicability to the case of hail.

## 2. Experiments

Measurements were conducted at 3.22 and 9.67 cm on a set of 11 ice spheroids and another set of 27 spheroids of Stycast Hi K.[2] Throughout the centimeter band and at 0C, ice has a complex refractive index $m=n-i\kappa=1.78-2.4\times10^{-3}i$ (Gunn and East, 1954). In order to simulate ice, we selected the stycast material, for which $n=1.73\pm0.04$. The absorption coefficient of this material is less than $1.7\times10^{-3}$. Thus, the stycast should behave almost identically to ice. The two way loss through plane slabs of ice and stycast would be 0.041 and 0.029 db cm$^{-1}$, respectively, at 3.22-cm wavelength and 1/3 these values at 9.67 cm. Thus the losses are negligible for the particle sizes of concern here.

The measurements were made using the back-scatter facilities of the Electromagnetic Radiation Laboratory, Air Force Cambridge Research Laboratories, at Ipswich, Mass. The measurement system is described in detail by Gorr (1959). For the ice particles, we used a bistatic system with transmitting and receiving horns mounted adjacent to one another. For the stycast particles, we utilized a monostatic system. Both systems are outdoors.

The parameters of the bistatic experimental arrangements for the ice measurements are summarized in Table 1. Note that the axes of the receiver horns were slightly off from the exact back-scatter direction. Also, the receiver horns intercepted energy over angular dimensions of 2 to 3 deg as viewed from the target position. The same receiver horns were later used in the monostatic measurements of the stycast particles. However, the distance between horn and target was reduced to 22 ft at 3.22 cm and to 10.5 ft at 9.67 cm. Thus, at 9.67 cm, the angular dimensions of the horn were then $4.7\times6.7$ degrees as viewed from the target. In other words, the receiver is averaging slightly over a region of the particle's radiation pattern.

In either the monostatic or bistatic system, the signals from the target mount and background are balanced out prior to insertion of the target to be measured. Introduction of the target creates an unbalance signal which is proportional to its cross section. This is amplified by a receiver and applied to a recorder which utilizes this signal and angular information from the target rotating device to give a rectangular plot of the target cross section as a function of rotation.

Prior to each target measurement, the signal level corresponding to that of a standard metal sphere was recorded to provide an absolute scale for target cross section. Comparison of the measured cross sections of the metal spheres to theoretical values indicates that the absolute accuracy of the measurements is generally within $\pm1$ db except near noise level. Occasionally, however, unknown disturbances in the field caused greater errors. Relative accuracy during any one rotation is also of the order of $\pm1$ db.

The targets were placed on a polyfoam column split at the top to provide a firm hold. The polyfoam column in turn is attached to a mount and rotating device. A tilted wood baffle lined with microwave absorbing material was used to reduce reflections from the mount and rotator.

A theodolite positioned just behind the transmitting horn was used to align each oblate spheroid so that its major axis was vertical. Since the ice particles had to be handled rapidly, it was not always possible to obtain perfect vertical orientation; occasional deviations up to 5 deg were noted. The stycast particles could be handled more leisurely and vertical orientation was good to $\pm3$ deg.

The ice particles were stored in a cold box packed with

TABLE 1. Parameters of the bistatic systems used in the ice scatter measurements.

| | |
|---|---|
| Distance—horns to target | 25 ft |
| *Wavelength—9.67 cm* | |
| Horn dimensions | |
| Transmitter | $9''(E)\times10.5''$ |
| Receiver | $10.25''(E)\times14.75''$ |
| Horn spacing—center to center | 13.5″ |
| Angular deviation of receiver horn axis from back-scatter direction | 2.6 deg |
| Angular dimensions of receiver (from target) | 2.0 deg $(E)\times2.8$ deg |
| *Wavelength—3.22 cm* | |
| Horn dimensions | |
| Transmitter and receiver | 10.25 deg $(E)\times12.75''$ |
| Horn spacing—center to center | 14.0″ |
| Angular deviation of receiver horn axis from back-scatter direction | 2.7 deg |
| Angular dimensions of receiver (from target) | 2.0 deg $(E)\times2.4$ deg |

* $E$ signifies the plane of the electric field.

[1] Harper, W. G., 1960: Radar back-scattering from oblate spheroids. Unpublished manuscript, Meteorological Office, London, 10 pp.

[2] Manufactured by Emerson and Cuming, Inc., Canton, Mass.

Unauthenticated | Downloaded 06/28/22 12:35 AM UTC

dry ice until ready for use. Each particle was weighed to the nearest 0.1 gram and its major and minor axes measured to the nearest 0.1 cm before the measurement. The entire measurement procedure took between three and five minutes during which time the ice remained at temperatures below 0C.

The ice spheroids had been frozen in accurately machined, hollow oblate plasticene molds. While the thinner oblates were very well shaped, minor distortions were observed on the thicker ones. The stycast particles were machined and were more nearly perfect oblates; however, close examination also showed minor asymmetries. With a perfectly oriented perfect spheroid, the scatter pattern should reproduce exactly every 90 deg of rotation. This was generally the case; and the four 90-deg sections repeated to within ±1 db. However, if the particle was distorted, or not perfectly oriented, or not centered on the axis of rotation, small asymmetries in the recorded patterns were observed. In any case, since the system balance could not be maintained to better than ±0.5 db, the final pattern for each particle was obtained by a linear average of the four 90-deg sections of record. Where the signals dropped to noise level, the corresponding section of record was omitted from the average.

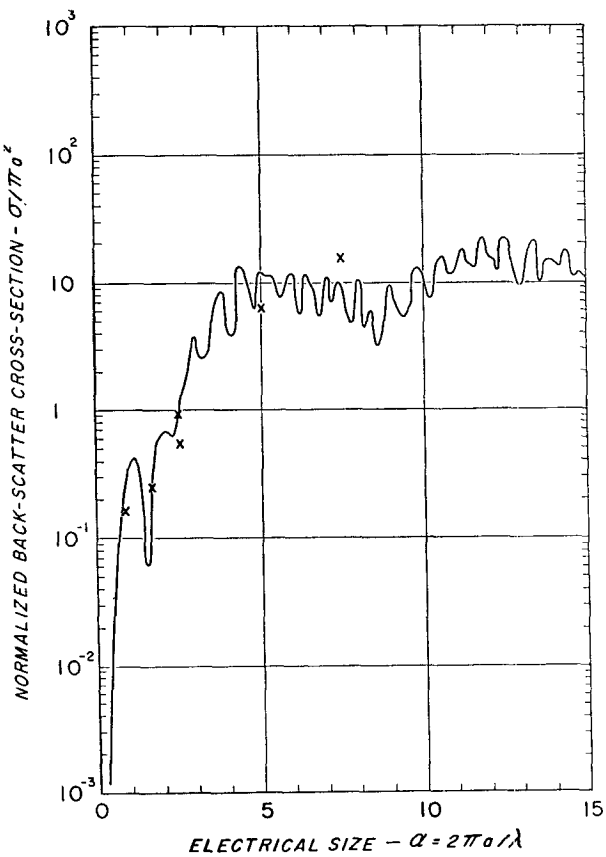


FIG. 1. Normalized radar cross sections ($\sigma/\pi a^2$) measured for stycast spheres with $m=1.73$ (crosses) compared to theoretical scatter cross sections of ice, $m=1.78$ (curve) as a function of $\alpha=2\pi a/\lambda$. The three lowest points are at 9.67 cm; the others at 3.22 cm.

In the measurements the large circular face always appears at the 90-deg position and the small face at the 0-deg position. Obviously, the circular face should present the same cross section to horizontal and vertical polarization. Agreement on the two polarizations was generally within ±1 db. Wherever the large face cross sections differed for the two polarizations, the true 90-deg value was taken as the average and the adjacent 20-deg section of record on each polarization was adjusted slightly to make a smooth transition to the average 90-deg value.

## 3. Results

### *3.1 Stycast particles*

In order to determine whether the small difference in refractive index between stycast ($n=1.73$) and ice ($n=1.78$) is significant, we have plotted the measured normalized radar cross sections of the three stycast spheres at the two wavelengths in Fig. 1 with respect to the established theoretical back-scatter curve for ice (after Herman and Battan, 1961a). The agreement is quite reasonable and justifies the use of the stycast to simulate ice. The minor discrepancies which appear in Fig. 1 (and also in the top patterns of Figs. 2a–b) are probably due to a combination of experimental error and the actual difference between stycast and ice.

The patterns for all the stycast particles are presented in Figs. 2a and 2b in order of increasing $2a/\lambda$. Fig. 2a represents the 9.67-cm data; Fig. 2b shows the 3.22-cm data for the same particles. However, barring discrepancies resulting from differences in measuring equipment and arrangement, wavelength effects should be negligible since the refractive index of stycast is the same at both. Only the parameter $2a/\lambda$ is important.

For "perpendicular" polarization, the polarization is perpendicular to the major axis of the particle, which is the axis about which it is being rotated; thus, in this mode, the particle dimension in the direction of polarization is changing from a maximum at 90 deg (circular or large face) to a minimum at 0 deg (small face). For "parallel" polarization, the polarization is parallel to the major axis; thus, while the projected area is changing as the particle rotates, the dimension along the direction of polarization remains constant. In each figure, the curves represent the recorded patterns, while the large tick mark at the left represents the cross section of an equivolume sphere, assuming that stycast spheres scatter identically to ice. The ordinate is in decibels relative to 1 cm².

Let us examine the smallest particles ($2a/\lambda=0.263$) as indicated in Fig. 2a. These show the simplest behavior. For polarization parallel to the major axis these particles show very little sensitivity to orientation

Unauthenticated | Downloaded 06/28/22 12:35 AM UTC

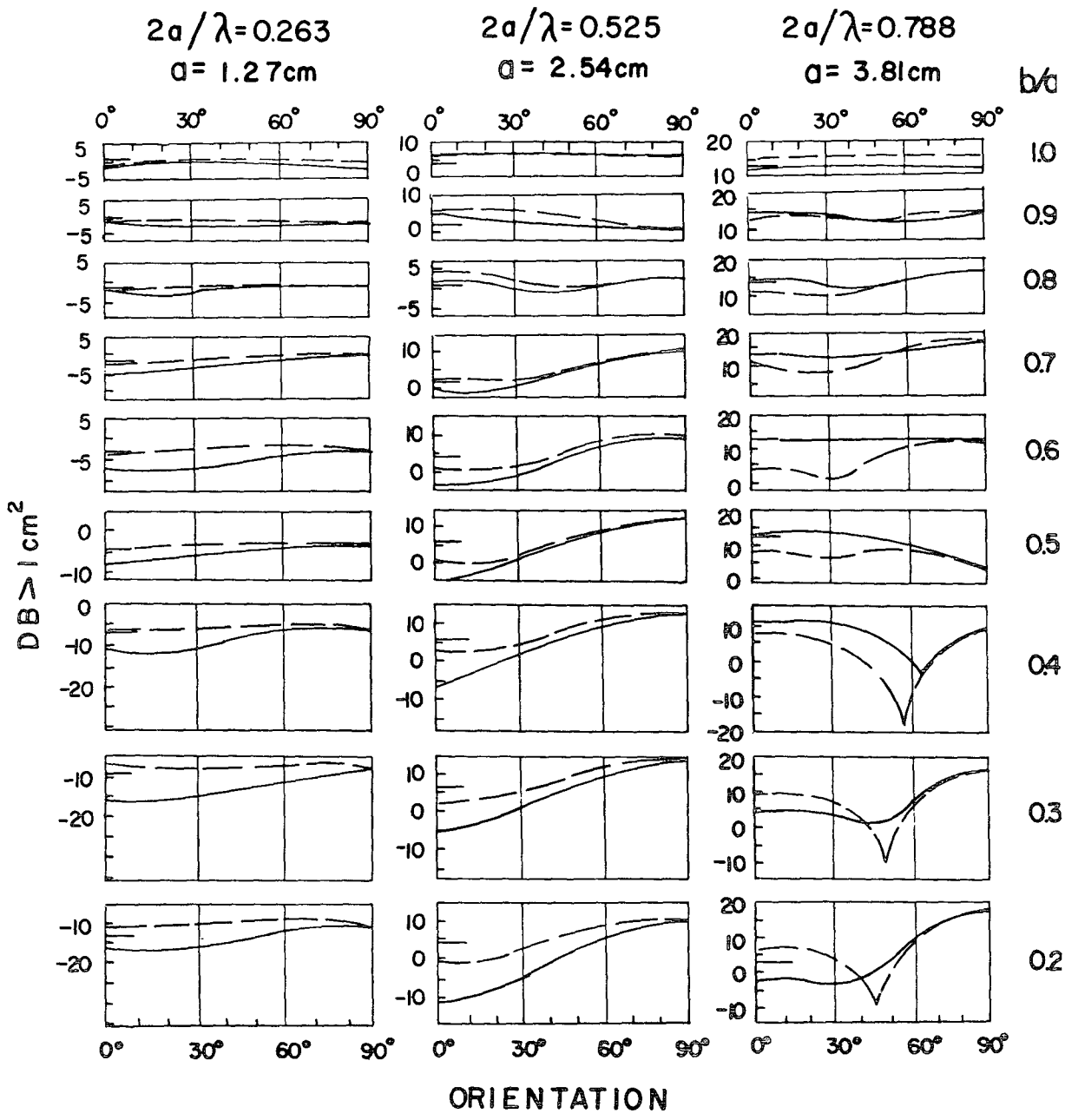


FIG. 2a. Variation of the back-scatter cross-section of stycast oblate spheroids as a function of angular aspect, from circular face (90 deg) to small elliptical face (0 deg) for axis/diameter ($b/a$) ratios from 1.0 to 0.2 measured at $\lambda=9.67$ cm. Particles are rotated around their diameters. Solid curve: polarization perpendicular to diameter of rotation; dashed curve: polarization parallel to diameter. Ordinate is decibels relative to 1 cm². Long tick on left margins represents the cross section of an equivolume sphere assuming the stycast scatters like ice.

regardless of ellipticity. The overall variation over the 90-deg rotation is generally less than 2.5 db with the greatest cross section occurring on or close to the large face. As the particles deviate increasingly from spheres, however, the cross section relative to an equivolume sphere increases. The maximum enhancement is about 4 db for $b/a=0.2$ at large face.

With polarization perpendicular to the major axis, or parallel to the minor axis the variation in back-scatter cross section with orientation is noticeably greater, with a smooth monotonic decrease from a maximum at the large face (90 deg) to a minimum at the small face (0 deg).

The behavior for these particles with small electrical

Unauthenticated | Downloaded 06/28/22 12:35 AM UTC

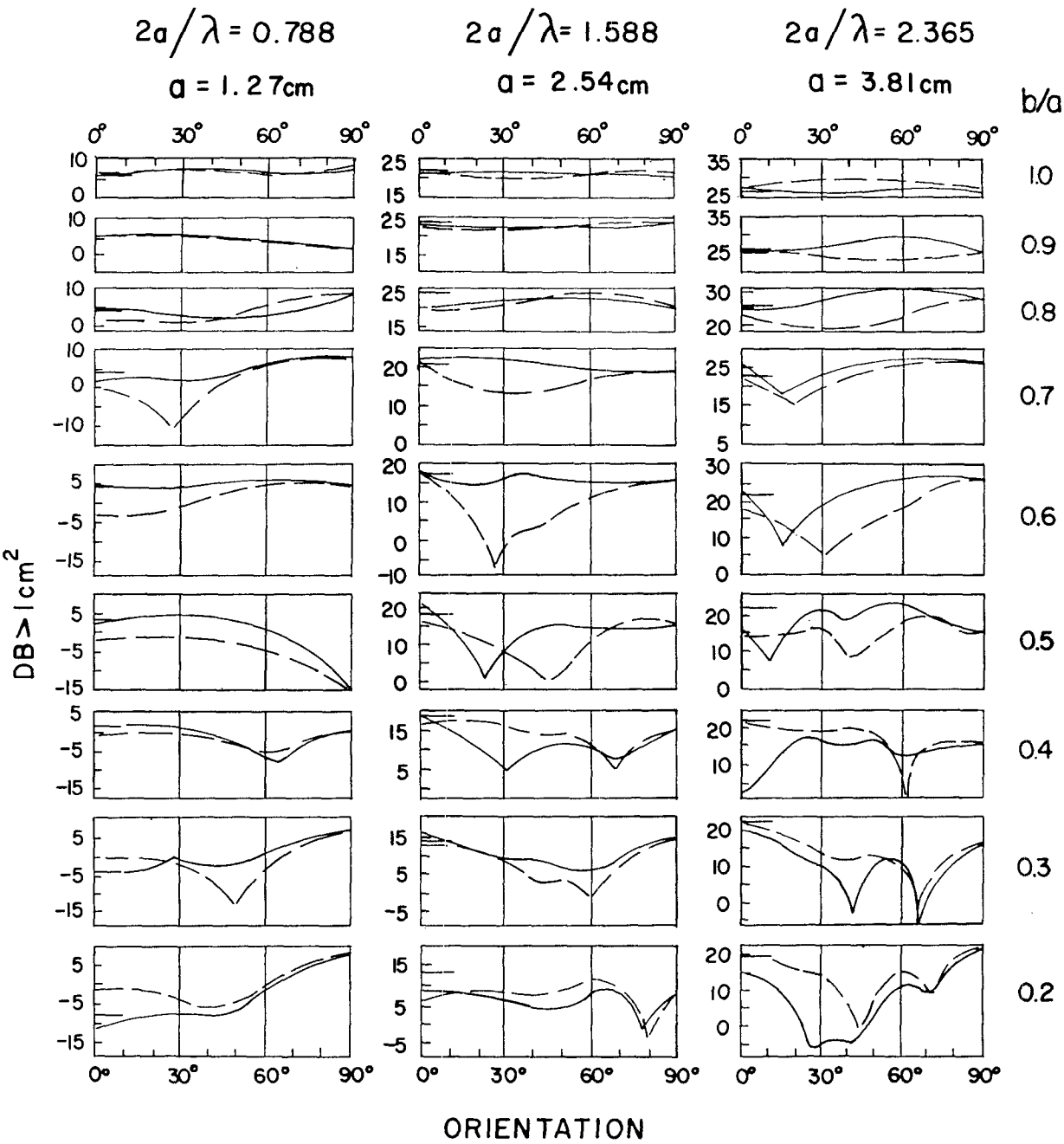


FIG. 2b. Same as Figure 2a, but measured at $\lambda = 3.22$ cm.

size ($2a/\lambda = 0.263$) is very similar to that predicted by the Gans theory for small oblate particles (Atlas, Kerker and Hitschfeld, 1953). In Fig. 3 we have plotted the ratio of the cross section of the oblate to that of the equivolume sphere as a function of axis-to-diameter ratio. For the small face there are two curves, for polarization parallel and perpendicular to the major axis; for the large face there is obviously only one curve.

In addition, we have plotted the curves predicted by the Gans theory in Fig. 3a, as calculated by Atlas *et al.* (1953). In this theory, for constant ellipticity, the dipole moment induced in the scatterer is a function only of the dimension of the particle along the direction of polarization and the volume of the particle. Thus, the back-scatter cross section for the small face (0 deg) with polarization parallel to the major axis is the same

Unauthenticated | Downloaded 06/28/22 12:35 AM UTC

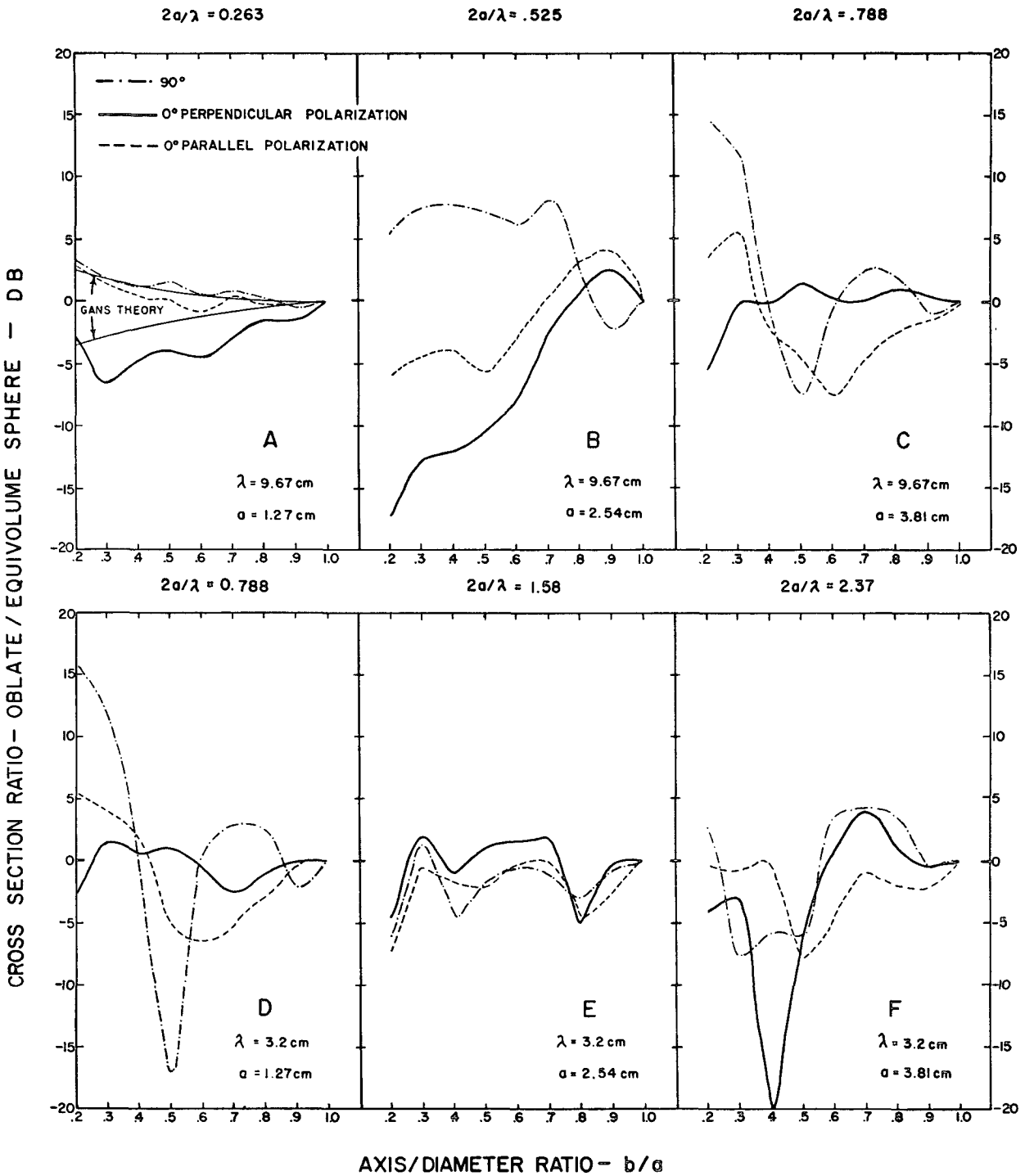


FIG. 3. Cross sections of stycast oblate spheroids relative to those of equivolume spheres in decibels, plotted versus axis/diameter ($b/a$) ratio, for circular face (90 deg)—dot-dash curves; small face, parallel polarization—dash curves; small face, perpendicular polarization—solid curves. A—$2a/\lambda=0.263$; B—$2a/\lambda=0.525$; C, D—$2a/\lambda=0.788$; E—$2a/\lambda=1.58$; F—$2a/\lambda=2.37$. Thin solid curves in A refer to the Gans theory (see text). A, B, C—measured at $\lambda=9.67$ cm; D, E, F—measured at $\lambda=3.22$ cm.

Unauthenticated | Downloaded 06/28/22 12:35 AM UTC

as that for the large face (90 deg). Within the experimental error, the measured cross sections are also identical at 90 deg and 0 deg, parallel. Furthermore, they fall close to the predicted Gans curve. Deviations up to about 2 db from the Gans curve may not be significant because of a combination of experimental errors and the use of the ice sphere scatter data to represent the cross section of spheres of stycast material. For the small face (0 deg) with perpendicular polarization, the measured values fall slightly below the predicted Gans curve, although the trend is similar.

We conclude that oblate spheroids with $2a/\lambda = 0.263$ scatter nearly as predicted by the simple Gans theory. The implication is that this is approximately the maximum electrical size of the particles at which this simple theory is applicable.

The situation becomes somewhat more complex as the particles become larger. For example, in Fig. 2a with $2a/\lambda = 0.525$, we see that the effect of particle orientation is amplified. For particles with $b/a \leq 0.7$, we find the maximum cross section when viewing the large face, with values 6 to 8 db greater than the equivolume sphere, and a smooth decrease to a minimum when viewing the small face. The decrease of cross section as the small face comes into full view (0 deg) is greater with perpendicular polarization than with parallel polarization. At 0 deg the degradation ranges from 2 to 17 db below the equivolume sphere for perpendicular polarization, but only down to 6 db for parallel polarization.

The patterns are altered, however, for $b/a > 0.7$. At $b/a = 0.8$, maxima occur at both 0 deg and 90 deg, while at $b/a = 0.9$ the maximum is reversed and appears when viewing the small face. In this position the enhancement over an equivolume sphere may be a few decibels.

As we increase the particle size further to $2a/\lambda = 0.788$ (Figs. 2a and 2b), the complexity of the patterns increases further. For this electrical size we have two sets of measurements, the 7.62-cm diameter particles at 9.67 cm (Fig. 2a) and the 2.54-cm particle at 3.22 cm (Fig. 2b). Agreement between the two is generally good and gives us extra confidence in the measurements. However, with one exception ($b/a = 0.7$ at 3.22 cm, Fig. 2b), the minima are sharper at the longer wavelength. The only general remark that can be made about the patterns is the appearance of one minimum at an intermediate orientation angle, whereas with the smaller particles the minimum occurs at one extreme or the other.

In Figs. 3c and 3d are plotted the cross sections at the extreme angles (0 deg, 90 deg) relative to equivolume spheres for this set of particles. Both Figs. 3c and 3d are similar in appearance, and with minor exceptions, in magnitude as well. When viewing the large face (90 deg), enhancement over the equal sphere is no longer a general occurrence as with the smaller sizes. Instead, the curves oscillate widely as a function of $b/a$. Slight degradation occurs for $b/a = 0.9$; slight enhancement occurs between $b/a = 0.6$ and 0.8, then strong degradation near 0.5 and a reversal to strong enhancement at $b/a < 0.4$. The period of these oscillations in $2\pi b/\lambda \approx 1$, very similar to that for the oscillations in the back-scatter from ice spheres. This suggests that when the radiation is incident on the large face the crucial dimension, electromagnetically, is the particle depth along the direction of propagation. Since the two way electrical phase difference between the front and back surface reflections is $4bm2\pi/\lambda$ along the axis of symmetry, the oscillation period in $b/a$ (for this particle size) should be $\Delta(b/a) = 0.37$ if we consider simple interference between the axial reflections from these two surfaces. This is not in bad accord with the data, considering that observations are available only at intervals $\Delta(b/a) = 0.1$.

For the small face viewed with polarization parallel to the major axis (0 deg, parallel, in Figs. 3c, d) the cross sections are generally less than those of equivolume spheres except at very small values of $b/a$. On the other hand, at 0 deg, perpendicular, the cross sections are generally approximately equal to those of equivolume spheres. (The 9.67-cm data show slight enhancement while the 3.22-cm data show minor degradation. Since wavelength should make no difference, the conclusion must be that the 0 deg, perpendicular, cross sections are virtually equal to those of equivolume spheres.) An exception again occurs for $b/a = 0.2$ which shows a smaller than sphere cross section at both wavelengths.

This behavior is an interesting reversal from that found for the smaller particles, where the small faces showed greater cross sections with parallel than with perpendicular polarization.

We proceed to the next larger size in Figs. 2b and 3e where $2a/\lambda = 1.588$. The pattern complexity is even greater than previously. Intermediate minima are the rule with the exception of the two ellipsoids nearest to spherical in shape. Indeed in some instances, two intermediate minima occur. At the extreme orientations, both Figs. 2b and 3e show that the cross sections are generally, for most practical purposes, equal to those of equivolume spheres. Significant degradation occurs at both extremes and polarizations for $b/a \approx 0.8$ and 0.2. When viewing the small face, perpendicular polarization gives slightly greater cross sections than parallel polarization.

Finally, Figs. 2b and 3f pertain to the largest electrical size with $2a/\lambda = 2.37$. Sharp minima intermediate to the extreme orientations again occur, and double intermediate minima now appear at the smaller $b/a$'s Full face cross sections are slightly enhanced for $b/a \geq 0.6$, but degraded for smaller $b/a$ with respect to those of equal spheres. Small face cross sections are usually smaller than those of equivolume spheres. An exception is the particle with $b/a = 0.7$ which shows

Unauthenticated | Downloaded 06/28/22 12:35 AM UTC

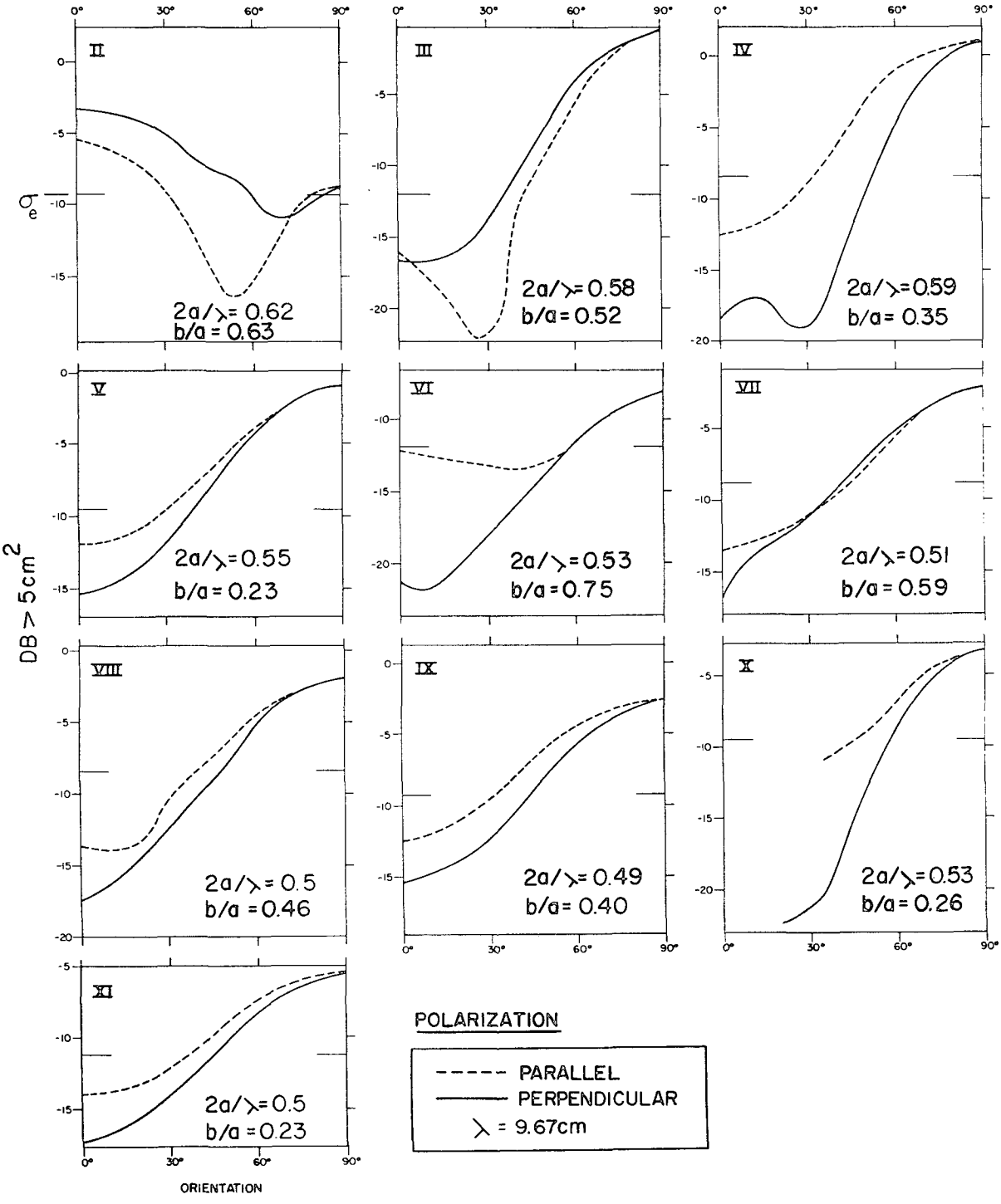


FIG. 4a. Same as Fig. 2a but for ice oblate spheroids. Electrical sizes ($2a/\lambda$) and axis/diameter ratios are indicated in the lower right hand corner of each diagram. Ordinate is in decibels relative to 5 cm². Solid curves—polarization perpendicular to diameter around which particles are rotated; dashed curves—polarization parallel to that diameter. 90 deg—large circular face in view; 0 deg—small elliptical face in view. Large tick marks on both sides of each diagram indicate the cross section of an equivolume sphere. Measured at $\lambda$=9.67 cm.

Unauthenticated | Downloaded 06/28/22 12:35 AM UTC

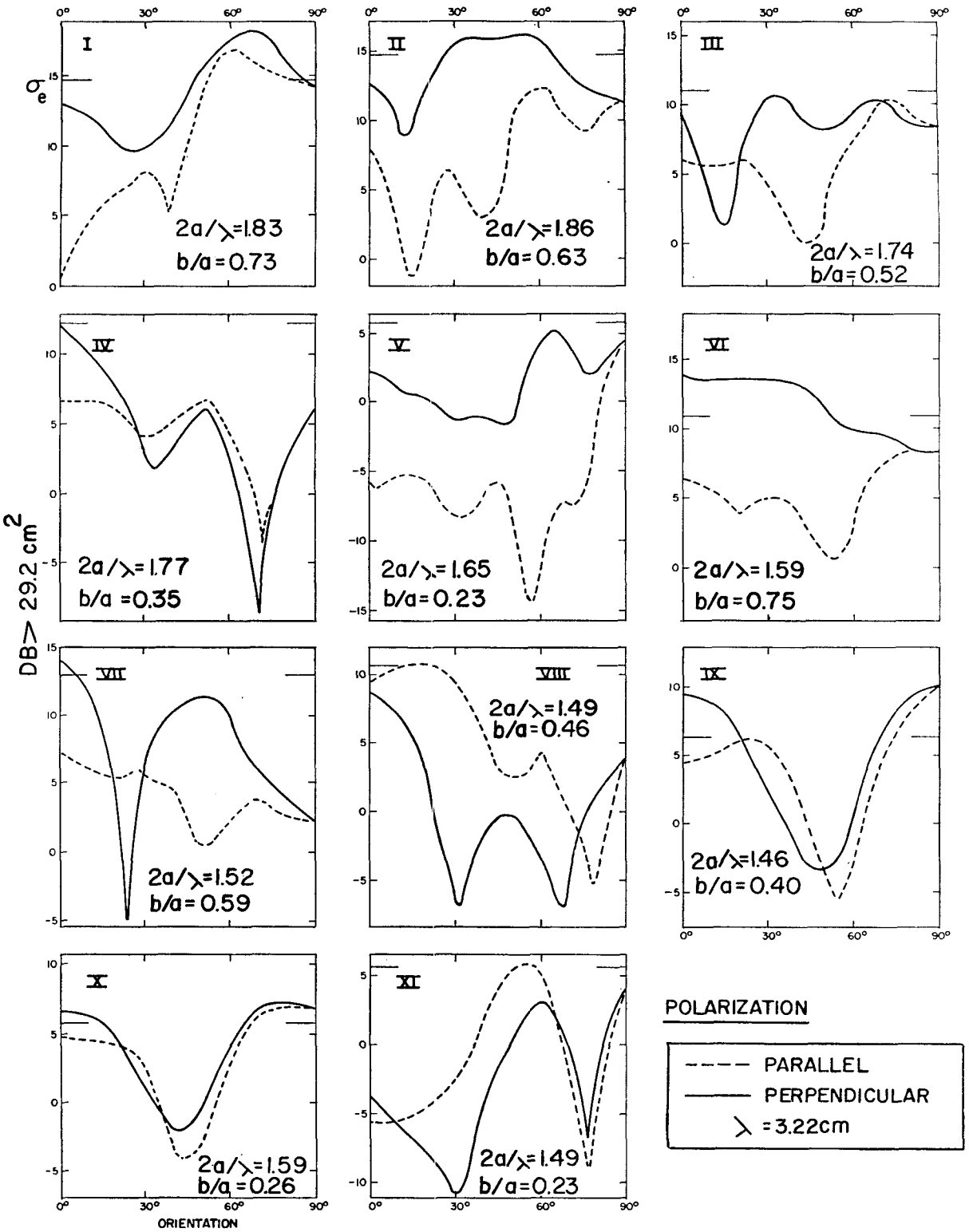


FIG. 4b. Same as Fig. 4a but measured at $\lambda = 3.22$ cm. Ordinate is decibels relative to 29.2 cm².

Unauthenticated | Downloaded 06/28/22 12:35 AM UTC

an enhancement of several decibels when the small face is viewed with perpendicular polarization. For $b/a \geq 0.5$, perpendicular polarization is again superior to parallel polarization.

### 3.2 *Ice particles*

A number of measurements were also conducted with ice oblate spheroids. These data were previously reported by Atlas and Wexler (1961). However, the conclusions of the latter paper must be altered in the light of the more comprehensive stycast data. The ice data are again presented here for comparison to the measurements with stycast. Despite the greater difficulties in making perfect oblate ice spheroids and in orienting them properly, the results are generally quite comparable to those with stycast. They are shown in Figs. 4a and 4b. Note that the cross sections are in decibels above a 5 cm$^2$ reference in Fig. 4a and a 29.2 cm$^2$ reference in Fig. 4b. Also, the level of the equivolume sphere is indicated by large horizontal tick marks on both sides of each diagram.

The data in Fig. 4a, taken at 9.67-cm wavelength, have values of $2a/\lambda$ ranging from 0.49 to 0.63. Thus, they may be compared most closely to Fig. 2a with $2a/\lambda = 0.525$. The patterns are seen to be very similar for similar values of $b/a$. In Fig. 5a we have superimposed the perpendicularly polarized pattern of particle IX from Fig. 4a on that from Fig. 2a with the same ellipticity ($b/a = 0.4$). The difference in the major axes (4.7-cm ice versus 5.08-cm stycast) probably accounts for the small deviations in their scatter patterns. As in the case of stycast, these small particles ($\simeq \lambda/2$) generally show cross sections greater than those of equivolume spheres when their large faces are viewed, and smaller than equal spheres when their small faces are in view. The variation is generally smooth and monotonic. An important exception to this general behavior is the largest particle (II) , with $2a/\lambda = 0.62$ and largest $b/a$(0.63). This one shows a maximum cross section on its small face with enhancements of about 6 and 4 db for perpendicular and parallel polarization, respectively. This enhancement on the small face is greater than any found with the stycast particles (Figs. 3b and 3c); however, ice particle II has a value of $2a/\lambda$ intermediate to those of Figs. 3b and 3c for stycast. It appears that maximum enhancement of the small face may occur with $2a/\lambda \simeq 0.62$ when $0.6 < b/a < 0.9$.

Fig. 4b presents the 3.22-cm measurements which are roughly comparable to those of Fig. 2b. In Fig. 4b $2a/\lambda$ ranges from 1.46 to 1.86 and the patterns have a complexity corresponding to this size. Agreement with the measurements for stycast oblates of similar size and ellipticity is fairly good. This is illustrated in Fig. 5b where a comparison is made between the perpendicularly polarized patterns for ice particle VIII with

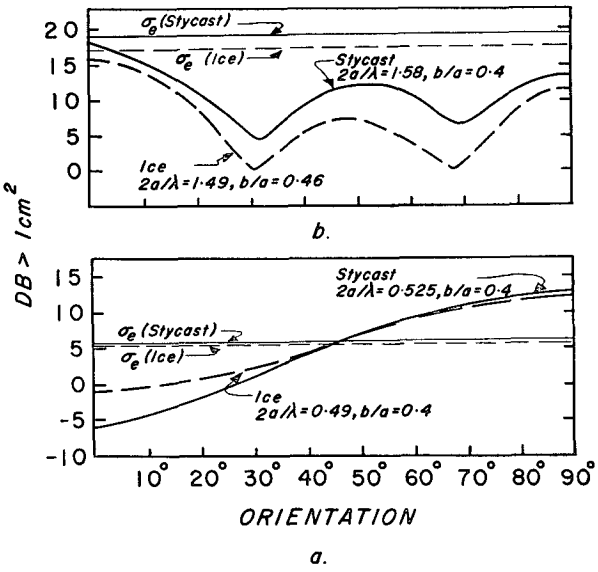


FIG. 5. Comparison of perpendicularly polarized back-scatter patterns for ice and stycast of similar sizes and shapes (as indicated) taken from Figs. 2 and 4. Horizontal lines correspond to equi-volume spheres.

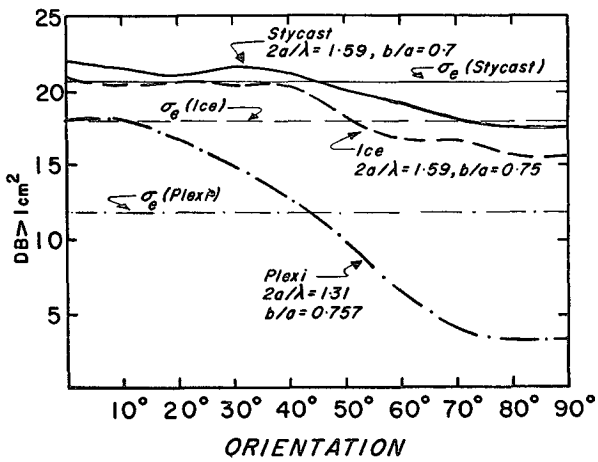


FIG. 6. Comparison of the perpendicular polarized patterns for ice and stycast (from Figs. 2 and 4) and plexiglass of approximately similar shapes and sizes (as indicated). Plexiglass data are due to Harper (1960). All show enhancement of 0 deg (small face). Horizontal lines correspond to equi-volume spheres.

$2a/\lambda = 1.49$, $b/a = 0.46$ and the stycast particle from Fig. 2b with $2a/\lambda = 1.58$, $b/a = 0.4$. In general, the cross sections with perpendicular polarization fall close to those of equivolume spheres at both small (0 deg) and large (90 deg) faces, but the parallel polarization may be significantly degraded on the small face. The small faces of particles VI and IX show significant enhancements with respect to equivolume spheres when viewed with perpendicular polarization. The enhancement shown by particle IX in Fig. 4b is comparable to that shown for $b/a = 0.3$ in Fig. 2b. Particle VI is meteoro-

Unauthenticated | Downloaded 06/28/22 12:35 AM UTC

logically more important since its $b/a=0.75$, a fairly common shape for oblate hailstones.

Since the question of possible enhancement of the small face cross sections is of vital importance to the interpretation of radar observations of hailstorms, Fig. 6 presents a direct comparison between the perpendicularly polarized patterns for ice particle VI ($2a/\lambda=1.59$, $b/a=0.75$), the nearest stycast particle ($2a/\lambda=1.59$, $b/a=0.7$), and a plexiglass oblate ($2a/\lambda=1.31$, $b/a=0.757$), the latter as measured by Harper.[3] All the patterns are similar and show enhancement of the small face cross section by these amounts: plexiglass, 6.3 db; ice, 2.9 db; stycast, 1.4 db. Thus, we can be confident that these exceptional particles do indeed show some enhancement on their small faces. The plexiglass particle has an electrical size intermediate to any of the ice or stycast particles which we measured. Thus, we cannot be sure that such large enhancements would not be observed with ice of identical size, although nowhere in Fig. 3 do we observe such great enhancement of the small face. The large difference in refractive index between plexiglass (1.61) and ice (1.78) makes us doubt that such large enhancement will be observed with ice of identical size and shape.

### 3.3 *Circular polarization cancellation ratios*

It is well known that the use of circular polarization reduces the echo from raindrops significantly. The ratio of echo power on circular polarization to that on linear is the cancellation ratio. The more nearly spherical the particles are, the larger the cancellation. Newell, Geotis and Fleisher (1957) report cancellation ratios for rain ranging from $-12$ to $-20$ db, with an average of about $-15$ db. The question arises as to whether or not the non-spherical nature of hailstones will permit distinguishing hail from rain by the difference in cancellation ratios.

Since a circularly polarized wave may be synthesized from equal horizontally and vertically polarized waves in time and space quadrature, it can be seen that a particle such as a sphere which scatters equally to both forms of linear polarization will produce the greatest cancellation ratios. With a perfectly circular wave the cancellation would be infinite. In practice, however, it is difficult to attain an antenna with perfect circularity, and so, cancellation ratios of $-20$ db or better may be associated with perfect spheres. Unfortunately, even if the particles are non-spherical, but for some reason their cross sections appear nearly equal on both linear polarizations, they will produce large cancellation ratios just like spheres. Obviously, a number of our oblate particles behave in this manner. Nevertheless, it is worthwhile to compute the expected cancellation ratios.

Since oblate hailstones indicate growth while falling with their largest dimension horizontal, we shall consider that such particles are perfectly oriented in this way in nature. Viewing these stones from below, they will appear circular and the cancellation ratios will always be infinite. Also, since most storms will be viewed from a great distance, the only case of practical interest is that in which the radar views their small elliptical faces (i.e., the 0 deg orientation in Figs. 2 and 4). From this aspect the incident linear polarization will always be parallel to one of the particle axes, and the back-scatter will be polarized completely in the direction of the incident polarization. Also, with the assumed orientation and aspect, horizontal polarization will correspond to parallel polarization in our measurements, and vertical to perpendicular polarization.

With these assumptions it may be shown that

$$P_c/P_L=(1-2\chi^{1/2}+\chi)/2, \tag{1}$$

where $P_c$ represents the echo power on circular polarization and $P_L$ is that on linear polarization. When $P_L$ is vertically polarized, $\chi$ represents the ratio $P_H/P_V$ (or the ratio of the measured cross sections on the two linear polarizations); when $P_L$ is horizontally polarized $\chi=P_V/P_H$. Obviously,

$$10\ \mathrm{Log}P_c/P_H=10\ \mathrm{Log}P_c/P_V-10\ \mathrm{Log}P_H/P_V. \tag{2}$$

We have used the ratio of the measured cross sections on parallel and perpendicular polarizations to calculate the expected cancellation ratios. Another assumption implicit in this calculation is that all the particles in the scattering volume are of the same size, shape and orientation but that they are randomly distributed in phase distance from the radar so that the total echo power is directly proportional to the number of scatterers.

Table 2 lists the values of $10\ \mathrm{Log}P_H/P_V$, and the cancellation ratios $10\ \mathrm{Log}P_c/P_V$ and $10\ \mathrm{Log}P_c/P_H$ for all the stycast particles. Where $\chi=P_H/P_V$ is close to one ($10\ \mathrm{Log}\chi\approx 0$) the cancellation ratio calculated from equation (1) is extremely sensitive to errors in $\chi$. Thus, for all values of $|10\ \mathrm{Log}\chi|<1.4$ db we simply indicate that the cancellation ratio exceeds 20 db. As we would expect from the patterns observed in Fig. 2, only the electrically small particles ($2a/\lambda\leq 0.525$) exhibit a simple behavior. For these particles, the ratio of horizontal to vertical polarized signals increases fairly uniformly with decreasing $b/a$, and so the cancellation ratios decrease accordingly. Wherever the signal on either linear polarization is more than 7.6 db below the other, the cancellation ratio produced upon switching from the weaker linear polarization to circular will be positive; i.e., more signal will be received on circular polarization. Several positive values of $10\ \mathrm{Log}P_c/P_V$ are indicated for the smaller $(b/a)$'s. Using a cancellation ratio of 12 db as the smallest value characteristic of rainfall, we may then ascribe cancellations $\lesssim 10$ db to non-spherical particles such as hail. All such values are

[3] *Loc. cit.*

Unauthenticated | Downloaded 06/28/22 12:35 AM UTC

TABLE 2a. Horizontally oriented oblate spheroids, $\lambda=9.67$ cm. Ratio of horizontal to vertical polarized cross sections (10 Log $P_H/P_V$) and corresponding cancellation ratios, circular to linear polarization (10 Log $P_c/P_V$) and 10 Log ($P_c/P_H$) (decibels) ($c$=circular, $V$=vertical, $H$=horizontal).

| | $2a/\lambda=.263$ | | | $2a/\lambda=.525$ | | | $2a/\lambda=.788$ | | |
|---|---|---|---|---|---|---|---|---|---|
| $b/a$ | $P_H/P_V$ | $P_c/P_V$ | $P_c/P_H$ | $P_H/P_V$ | $P_c/P_V$ | $P_c/P_H$ | $P_H/P_V$ | $P_c/P_V$ | $P_c/P_H$ |
| 0.2 | 6.0 | *− 3* | *− 9.0* | 11.5 | *5.8* | *− 5.8* | 9.0 | *2.3* | *− 6.9* |
| 0.3 | 8.0 | *0.6* | *− 7.6* | 8.0 | *0.6* | *− 7.6* | 5.5 | *− 4.1* | *− 9.5* |
| 0.4 | 5.25 | *− 4.5* | *− 9.75* | 8.0 | *0.6* | *− 7.6* | −2.25 | −16.0 | −13.1 |
| 0.5 | 4.0 | *− 7.8* | −12.1 | 4.75 | *− 5.7* | −10.8 | −6.0 | *− 9.0* | *− 3* |
| 0.6 | 3.75 | *− 8.3* | −12.4 | 5.0 | *− 5.1* | −10.4 | −7.75 | *− 7.8* | *0.2* |
| 0.7 | 3.25 | *− 9.8* | −13.3 | 2.75 | −11.4 | −14.5 | −4.5 | −11.3 | *− 6.3* |
| 0.8 | 1.25 | <−20 | <−20 | 2.5 | −12.3 | −15.1 | −3.5 | −12.9 | *− 8.6* |
| 0.9 | 1.25 | <−20 | <−20 | 1.5 | −17.4 | −19.0 | −2.0 | −16.7 | −14.1 |
| 1.0 | 0 | <−20 | <−20 | 0 | <−20 | <−20 | 0 | <−20 | <−20 |

TABLE 2b. Horizontally oriented oblate spheroids, $\lambda=3.22$ cm. Ratio of horizontal to vertical polarized cross sections (10 Log $P_H/P_V$) and corresponding cancellation ratios, circular to linear polarization (10 Log $P_c/P_V$) and 10 Log ($P_c/P_H$) (decibels) $c$=circular, $V$=vertical, $H$=horizontal).

| | $2a/\lambda=.788$ | | | $2a/\lambda=1.58$ | | | $2a/\lambda=2.37$ | | |
|---|---|---|---|---|---|---|---|---|---|
| $b/a$ | $P_H/P_V$ | $P_c/P_V$ | $P_c/P_H$ | $P_H/P_V$ | $P_c/P_V$ | $P_c/P_H$ | $P_H/P_V$ | $P_c/P_V$ | $P_c/P_H$ |
| 0.2 | 8.25 | *0.9* | *− 7.35* | −2.75 | −14.5 | −11.75 | 3.5 | *− 8.6* | −12.1 |
| 0.3 | 2.5 | −12.3 | −14.8 | −2.50 | −15.1 | −12.60 | 2.0 | −14.1 | −16.1 |
| 0.4 | 1.5 | −17.4 | −18.9 | −0.75 | <−20 | <−20 | 21.0 | 17.0 | *− 4.0* |
| 0.5 | −5.75 | *− 9.2* | *− 3.45* | −3.0 | −13.8 | −10.8 | −1.25 | <−20 | <−20 |
| 0.6 | −5.75 | *− 9.2* | *− 3.45* | −1.75 | −17.4 | −15.65 | −5.25 | *− 9.9* | *− 4.65* |
| 0.7 | −2.5 | −15.0 | −12.5 | −2.0 | −16.7 | −14.7 | −4.75 | −10.8 | *− 6.05* |
| 0.8 | −2.25 | −16.0 | −13.75 | 0.5 | <−20 | <−20 | −3.0 | −13.8 | −10.8 |
| 0.9 | −0.25 | <−20 | <−20 | −2.0 | −16.7 | −14.7 | −1.5 | −19.0 | −17.5 |
| 1.0 | 0 | <−20 | <−20 | 0 | <−20 | <−20 | 0 | <−20 | <−20 |

italicized in Table 2. For the two smallest sets of particles $(-10\ \text{Log}P_c/P_V)\leq 10$ db when $b/a\lesssim 0.7$, while $(-10\ \text{Log}P_c/P_H)\leq 10$ db when $b/a\lesssim 0.4$. In other words, oriented non-spherical hail may be distinguished clearly from rain only when the particles are smaller than about $\lambda/2$ and $b/a<0.7$ and switching is from vertical to circular polarization. Since a cancellation of less than 10 db implies a ratio greater than 3.2 db between the two linear polarizations (1), switching from vertical to horizontal polarization should provide an equally useful means of identifying horizontally oriented oblate particles within the previously prescribed limits.

As the particles become larger ($2a/\lambda\geq 0.788$) we have already seen that, with few exceptions at the smallest $b/a$'s, vertical is superior to horizontal polarization. However, the differences are generally not so great as to produce cancellation ratios less than 10 db. Thus, when the particles are larger than about $3\lambda/4$, switching from either linear to circular polarization will not generally produce cancellation ratios greatly different from those to be expected in some extreme rainfalls.

In general, provided that differences in echo power of the order of 3 db can be accurately observed, the data of Table 2 indicate that it would be more informative (and simpler) to switch from vertical to horizontal polarization, at least insofar as horizontally oriented hailstones are concerned. A significant increase in echo in going from vertical to horizontal polarization would indicate the presence of oblate stones equal to or smaller than about $\lambda/2$; a significant decrease would generally imply oblate stones larger than $3\lambda/4$ since the shapes which produce the opposite effect have $b/a\leq 0.4$ and are uncommon in nature. Unfortunately, a small change in signals would not rule out the presence of large oblate stones.

Of course, any spread in orientation among the stones in the scattering volume would tend to obscure the above polarization effects. However, cross-polarized components may then become significant (Atlas *et al.*, 1953).

## 4. Discussion

While the accumulation of this fairly extensive encyclopedia of experimental data was necessitated by the lack of a suitable general theory, the complexity of the results and their inaccessibility to a straightforward physical interpretation is hardly satisfying. Perhaps we should not have been disappointed with the complexity of the results since the Mie theory produces equally complex results for dielectric spheres. Indeed, the Mie theory itself is not subject to a simple physical interpretation.

Only the smallest of our particles behaved in a simple manner closely approximated by the Gans (1912)

Unauthenticated | Downloaded 06/28/22 12:35 AM UTC

theory which is readily interpreted on physical grounds (Atlas *et al.*, 1953). However, the larger particles are not so readily understood. In the initial version of this paper, we attempted to explain their behavior in a qualitative way based on the geometric optics of back-scatter. However, very recent developments in the treatment of the back-scatter by dielectric spheres using methods of modified geometric optics by Thomas (1962) and by Atlas and Glover (1962) hold out the promise that spheroids can be treated similarly. Therefore, we shall omit a qualitative discussion in the hope that a more rigorous treatment will be available shortly.

## 5. Meteorological implications

Some of the more important implications of these results as they bear on the interpretation of radar observations of hailstorms are summarized below. Our assumptions are that: (1) the oblate hailstones are oriented with their major axes horizontal; (2) their shapes are limited to $0.5<b/a<1$; and (3) the angle between the radar beam and the normal to the small faces is not more than 10 deg. (Since most hailstorms will be viewed at some distance from the radar, we will omit the opposite case in which the storm is overhead and the stones are seen broadside.) Under these conditions, the following conclusions are valid:

(1) In general, the hailstone cross sections are equal to or less than those of equivolume spheres. When their diameters are smaller than about $0.5\lambda$, they scatter somewhat better on horizontal polarization than on vertical; the reverse is true for sizes larger than $0.5\lambda$.

(2) In a restricted range of size and ellipticity, oblate stones may scatter slightly better than equivolume spheres. Where such enhancement occurs, it is restricted to a few decibels, and then only when orientation is perfect. Furthermore, surface irregularities, which are characteristic of natural stones, will degrade their cross sections. Thus, it is not possible to attribute extraordinarily large hailstorm reflectivities to deviations from sphericity, at least in the case of dry hail viewed narrow end on. When the stones are wet and electrically small, their cross sections may be significantly enhanced on horizontal polarization and degraded on vertical polarization (Atlas *et al.*, 1953).

(3) Shape effects are rather sensitive to the stone's electrical size. Thus, a hailstone which appears "small" at 10-cm wavelength may be "large" at 3 cm. With 5-cm diameter stones, reflectivities at a wavelength of 10 cm may be significantly degraded with respect to those at 3 cm when $b/a\leq 0.7$; the reverse is true when $b/a>0.7$. Thus, hailstorm reflectivity profiles are not comparable from one wavelength to another.

(4) When the stones are electrically large ($2a/\lambda\gtrsim 2$) and $b/a\lesssim 0.8$, their cross sections on vertical polarization are fairly sensitive to orientation. Reflectivity will generally decrease from a maximum at 0 deg incidence (elevation angle) by a few decibels as the antenna is raised to 10 deg. (This is obviously restricted to short ranges.) This effect is opposite to that of the reflectivity maximum aloft (Donaldson, 1961) and therefore cannot be invoked to explain the latter phenomenon.[4] On horizontal polarization, reflectivity is much less sensitive to elevation angle. This is also true for stones with $b/a\geq 0.8$ on either polarization.

(5) The cancellation ratio produced by switching from linear to circular polarization depends upon the difference in hailstone cross sections on two orthogonal linear polarizations. If the two linear polarizations produce cross sections within $\pm 1.4$ db of each other, the cancellation ratio will exceed 20 db. However, even with nearly spherical raindrops, measured cancellation ratios range from about 12 to 20 db (Newell *et al.*, 1957). Thus, in order to distinguish hail from rain by circular polarization, the cancellation ratios must be less than about 10 db. This corresponds to a difference in the two linear polarizations of about $\pm 3$ db or greater. Unfortunately, for stones whose $b/a\geq 0.5$, the observed differences on vertical and horizontal polarization are not frequently in excess of 3 db, so that switching from linear to circular polarization will not generally permit differentiation of hail from the extreme rainfalls. As the various particles take up an increasingly broad spectrum of orientations, differences in polarization would have smaller and smaller effects.

(6) When the particles are electrically small, the Gans theory predicts greater polarization effects for water-coated ice spheroids than for dry ice (Atlas *et al.*, 1953; Labrum, 1953). These effects probably extend into the larger size regime as well. Since, at 3 cm, thinly coated ice spheres behave essentially as water drops (Herman and Battan, 1961b), it seems likely that polarization switching will permit recognition of wet oriented ice spheroids.

It is emphasized that all our previous conclusions pertain to dry ice, except where noted.

*Acknowledgments.* The authors are pleased to acknowledge their great appreciation to the Electromagnetic Radiation Laboratory, Air Force Cambridge Research Laboratories, for the use of their scatter facilities; and especially to B. B. Gorr, of that Laboratory, who meticulously conducted the experiments. G. K. Thompson, of Allied Research Associates, assisted invaluably in the manufacture of the ice spheroids. E. F. Duquette, of the same organization, and A. C. Chmela, of the Meteorological Research Laboratory, Air Force Cambridge Research Laboratories, were of great help in the data reduction and preparation of illustrations. Valuable discussions were held with Dr. R. M. Lhermitte, of AFCRL, and Dr. E. M. Brooks and S. Weiner, of Allied Research Associates.

[4] Unless we assume some preferred oblique orientation as might occur if the particles fall with their large faces perpendicular to the vector sum of their fall velocity, and horizontal wind velocity.

Unauthenticated | Downloaded 06/28/22 12:35 AM UTC

## REFERENCES


Atlas, D., M. Kerker and W. Hitschfeld, 1953: Scattering and attenuation by non-spherical atmospheric particles. *J. atmos. and terr. Phys.*, **3**, 108–119.

Atlas, D., W. G. Harper, F. H. Ludlam and W. C. Macklin, 1960: Radar scatter by large hail. *Quart. J. R. meteor. Soc.*, **86**, 468–482.

Atlas, D., and R. Wexler, 1961: Radar scatter by large non-spherical hail. *Proc. Ninth Weather Radar Conf.*, Boston, Amer. Meteor. Soc., pp. 272–279.

Atlas, D., and K. M. Glover, 1962: Back-scatter by dielectric spheres with and without metal caps. *Proc. Interdisciplinary Conf. on Electromagnetic Scattering*, New York, Pergamon Press, in press.

Donaldson, R. J., 1961: Radar reflectivity profiles in thunderstorms. *J. Meteor.*, **18**, 292–305.

Gans, R., 1912: Über die Form ultra mikroskopischer Goldteilchen. *Ann. Phys.*, **37**, 881–900.

Gorr, B. B., 1959: Air Force Cambridge Research Center radar cross section measuring equipment and range. Air Force Cambridge Research Center, Report No. AFCRC–TR–59–137, 30 pp. (ASTIA Document no. AD 214844).

Gunn, K. L. S., and T. W. R. East, 1954: The microwave properties of precipitation particles. *Quart. J. R. meteor. Soc.*, **80**, 522–545.

Herman, B. M., and L. J. Battan, 1961a: Calculations of Mie back-scattering of microwaves from ice spheres. *Quart. J. R. meteor. Soc.*, **87**, 223–230.

—— and ——, 1961b: Calculations of Mie back-scattering from melting ice spheres. *J. Meteor.*, **18**, 468–478.

Labrum, N. R., 1953: The scattering of radio waves by meteorological particles. *J. appl. Phys.*, **23**, 1324–1330.

Mathur, P. N., and E. A. Mueller, 1955: Radar back-scattering from non-spherical scatterers. Report of Investigation No. 28, Illinois State Water Survey Division, 85 pp. (Available at University Library, University of Illinois.)

Newell, R. E., S. G. Geotis and A. Fleisher, 1957: The shape of rain and snow at microwavelengths. Research Report No. 28, Mass. Inst. of Technology, Dept. of Meteorology, 103 pp. (Available from Library of Congress PB 142–064. Microfilm, $5.70; Photo, $16.80.)

Stevenson, A. F., 1953: Electromagnetic scattering by an ellipsoid in the third approximation. *J. appl. Phys.*, **24**, 1143–1151.

Thomas, D. T., 1962: Scattering by plasma and dielectric bodies. Ph.D. dissertation, Dept. of Electrical Engineering, Ohio State University. Also published as Rep. No. 1116–20 Antenna Lab., Dept. of Elec. Eng., Ohio State Univ. under Contract No. AF 19(604)–7270 (AFCRL–62–735), 97 pp.


Unauthenticated | Downloaded 06/28/22 12:35 AM UTC